Semicond. Sci. Technol. 7 (1992) 961–967. Printed in the UK

A novel mechanism for parallel conduction in GaAs–(Ga,Al)As heterojunctions

R M Kusters†§, T J B M Janssen†, C J G M Langerak†||, J Singleton†¶, J A A J Perenboom†, G A C Jones‡, D A Ritchie‡ and J E F Frost‡

† High Field Magnet Laboratory and Research Institute for Materials, University of Nijmegen, Toernooiveld, NL-6525 ED Nijmegen, The Netherlands
‡ Cavendish Laboratory, University of Cambridge, Madingley Road, Cambridge CB3 0HE, UK

Received 14 October 1991, in final form 25 February 1992, accepted for publication 18 March 1992

Abstract. GaAs–(Ga,Al)As heterojunctions often show parallel conduction after illumination with red light ($\hbar\omega > E_g$). A study of the parallel conduction occurring in planar doped GaAs–(Ga,Al)As heterojunctions with a superlattice buffer is presented. The samples studied are subject to parallel conduction by two different types of carrier. Transport measurements indicate the presence of a very large density of low-mobility carriers, while in addition the presence of some high-mobility carriers is indicated by the appearance of an additional dip in the far-infrared (FIR) transmission. The latter type of carrier is thought to form a secondary low-density two-dimensional electron gas weakly confined behind the superlattice buffer.

1. Introduction

One of the most attractive properties of modulation-doped GaAs–(Ga,Al)As heterojunctions is the very high electron mobility achieved in these structures, which can be exploited in transistors with very high switching speed. However, the performance of such a transistor (high electron mobility transistor, HEMT) is considerably reduced if there are more conducting paths than through the active layer of the two-dimensional electron gas (2DEG) [1]. The most probable cause of parallel conduction in GaAs–(Ga,Al)As heterojunctions is the presence of conduction band (CB) electrons in the (Ga,Al)As layer [1–3], and this depends on the doping parameters (doping concentration, spacer width, thickness of the (Ga,Al)As layer) and Al content of this layer [1]. The latter determines the CB potential discontinuity at the interface: it must be at least ≈ 0.3 to prevent parallel conduction. The discontinuity in the potential at the interface must be at least some tens of meV higher than the product of the spacer width and the interface electric field, which is proportional to the sum of the 2D carrier density and the depletion charge density. Parallel conduction occurs if there is a region in the (Ga,Al)As where the CB edge is lower than the Fermi energy E_F. Another important parameter determining the presence of parallel conduction is the density of ionized donors $n_D(z)$, which is proportional to the second spatial derivative dV_{CB}^2/dz^2 of the CB-edge potential (z is the direction perpendicular to the 2DEG). In our samples $n_D(z)$ has a very high and narrow peak at the position of the planar Si doping.

Parallel conduction can be a result of the persistent photoconductivity (PPC) effect [4], which leads to ionization of deep donor states (DX centres [5]), thus increasing the effective value of $n_D(z)$, which changes $V_{CB}(z)$ in the (Ga,Al)As and the electric field at the interface.

We have observed such an onset of parallel conduction in three MBE-grown heterojunctions after a certain amount of illumination with red light. These samples are different from conventional GaAs–(Ga,Al)As heterojunctions: the (Ga,Al)As layer is undoped except for a sheet of 5×10^{16} m^{-2} Si donors at a distance d from the interface; d is 5, 10 and 20 nm respectively in the

§ Present address: Royal Dutch/Shell Exploration and Production Laboratory, NL-2280 AB Rijswijk, The Netherlands.
|| Present address: University of Nottingham, Nottingham NG7 2RD, UK.
¶ Present address: Clarendon Laboratory, University of Oxford, Oxford OX1 3PU, UK.

0268-1242/92/070961+07$04.50

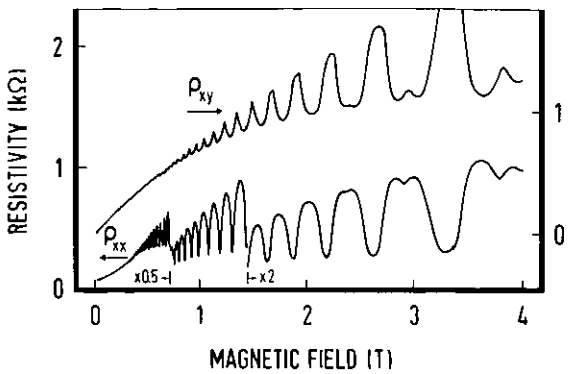

Figure 1. Typical traces of the diagonal and Hall resistivity observed in sample 3 after saturation of the carrier density. Due to strong parallel conduction, the Hall resistance ρ_{xy} is now dominated by SdH oscillations.

three different samples [6]. Furthermore, the samples have a 20 × (2.5 nm GaAs + 2.5 nm AlAs) superlattice buffer to prevent dopant migration from the substrate [7].

The paper is divided into two parts. Section 2 deals with the transport data from the three samples after strong illumination. The results are discussed in terms of conduction by two different types of carrier: the electrons in the 2DEG and the parallel-conducting electrons. Sections 3 and 4 treat the observation of an additional peak in the far-infrared (FIR) absorption of two of our samples; this peak appears after strong illumination. An explanation for this phenomenon in terms of parallel conduction by weakly confined electrons in a GaAs layer is given: we assume that the growth scheme is responsible for the presence of the weakly confined parallel-conducting electrons.

2. Magnetotransport: results and discussion

Parallel conduction in high-mobility heterojunctions is usually observed in magnetotransport in that the high-field Shubnikov–de Haas (SdH) minima no longer approach zero. Furthermore, the quantized Hall plateaux, usually observed in such high-mobility 2DEGs, are distorted. Figure 1 shows a set of $\rho_{xx}(B)$ and $\rho_{xy}(B)$ traces from sample 3 with a very large amount of parallel conduction. The behaviour is characterized by the fact that the minimum of the SdH envelope shows a quadratic magnetoresistance at relatively low fields, is approximately linear at intermediate fields, and tends to saturate at fields well above 20 T. As long as the parallel conduction is weak the distortion shows up as a dip at the high-field side of the Hall plateaux (without parallel conduction the Hall resistance increases monotonically as a function of field). In the case of strong parallel conduction (figure 1) the distortions have evolved into SdH-like oscillations with a sign opposite to the SdH oscillations in ρ_{xx}, and the Hall plateaux are so strongly distorted that they can no longer be recognized. This phenomenon can be explained by a mixing of ρ_{xx} and ρ_{xy} as a result of the short-circuiting of the voltages across the 2DEG by the parallel-conducting layer.

Table 1. Estimated densities (in m^{-2}) and mobilities (in $m^2\ V^{-1}\ s^{-1}$) of the 2DEG and the parallel-conducting carriers after saturation of the persistent photoconductivity effect.

Sample	N_s	$\langle\mu_{2DEG}\rangle$	$N_{\parallel cond}$	$\langle\mu_{\parallel cond}\rangle$
1	16.3×10^{15}	8.5	$\approx 50 \times 10^{15}$	≈0.07
2	11.1×10^{15}	52	$\approx 50 \times 10^{15}$	≈0.08
3	6.57×10^{15}	74	$\approx 50 \times 10^{15}$	≈0.09

The density N_s of the electrons in the 2DEG in each sample after saturation of the persistent photoconductivity was obtained from the period of the SdH oscillations; the results, accurate to ±1%, are shown in table 1. Approximate values of the 2DEG mobility $\langle\mu_{2DEG}\rangle$, and the mobility $\mu_{\parallel cond}$ and density $N_{\parallel cond}$ of the parallel-conducting carriers were deduced by applying the model of Kane *et al* [3]. The conditions required for the Kane model $\rho_{xy} = B/(N_s + N_{\parallel cond})e$ ($\rho_{xx}^2 \ll \rho_{xy}^2$ and $\mu_{\parallel cond} B \gg 1$) are only approximately satisfied, even at our maximum field of 20 T. $N_{\parallel cond}$ can therefore only be obtained approximately as its determination depends on a qualitative extrapolation of the data to higher fields. The values of the mobility given in table 1 also depend on the aspect ratios of the samples, and these could only be estimated (≈ 2 for sample 1 and ≈ 8/3 for samples 2 and 3).

The results in table 1 show that saturation of the persistent photoconductivity effect gives rise to a very large number of parallel-conducting carriers with a low mobility. The most probable origin of the majority of these carriers is the δ-doping layer with $N_{Si} = 5 \times 10^{16}\ m^{-2}$; the carriers are expected to reside in the neighbourhood of this layer so that they are scattered very strongly by the ionized Si donors, leading to the low mobility.

In magnetotransport it is difficult to distinguish the presence of more than one parallel-conduction channel. In a qualitative way, however, their presence can be elucidated by combining the transport results with far-infrared (FIR) transmission data: different types of carrier may have different effective masses, and several different cyclotron resonances will then be observed.

3. An additional far-infrared absorption peak

We have performed FIR transmission spectroscopy on samples 1, 2 and 3 [6]. An optically pumped molecular-gas FIR laser [8] has been used as a fixed-frequency source and the FIR transmission has been recorded as a function of field at ≈ 25 different laser energies. Carbon bolometers were used as detector.

In the samples used in this study the total number of electrons in the 2DEG can be increased so much that the Fermi energy is above the band edge of the first excited electric subband of the confining well potential, and more than one subband will then be occupied. In figure 2 the FIR transmission of sample 2 after saturation

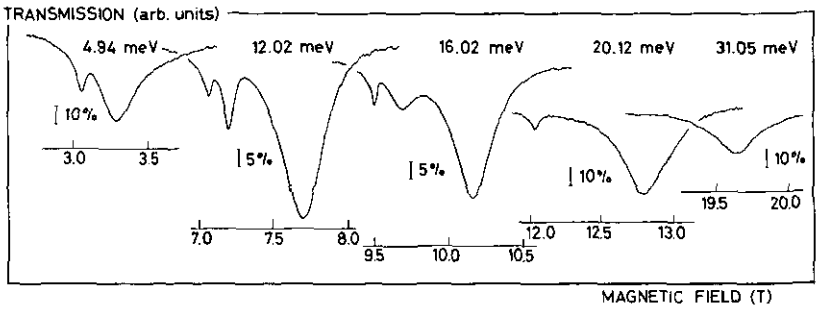

Figure 2. FIR transmission of sample 2 after saturation of the persistent photoconductivity effect at five different laser energies. Note the appearance of an additional resonance at $E_{FIR} = 12.02$ meV.

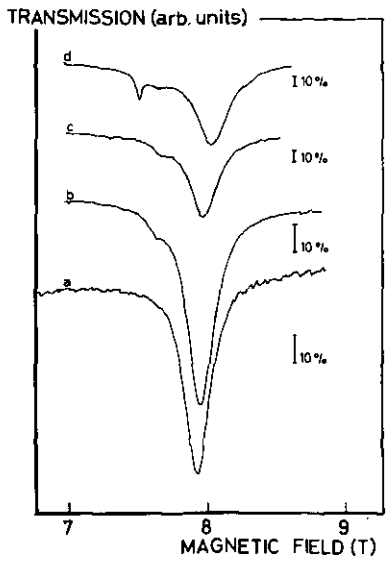

Figure 3. Evolution of the subband CRS and the T_3 resonance with successive increases of the 2DEG carrier density by bursts of red light; sample 2, $E_{FIR} = 12.85$ meV.

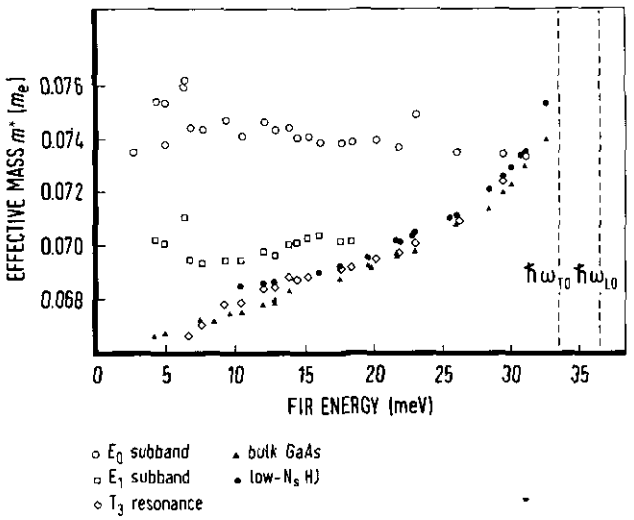

Figure 4. Effective masses extracted from the positions of the T_3 resonance as a function of FIR laser energy, and the subband effective masses m_0^* and m_1^*. Cyclotron masses of low-density heterojunctions [9] and bulk GaAs cyclotron masses [11, 12] are given for comparison; sample 2, $N_s = 1.16 \times 10^{16}$ m^{-2}.

of the carrier density is shown at five different laser energies. At an energy $E_{FIR} = 4.94$ meV we observe two dips due to CR: these originate from the carriers in the lowest and first-excited subband, and will be denoted as CR_0 and CR_1 respectively. At the 12.02 meV laser line, however, a *third* resonance, which will be denoted as T_3, is seen at the low-field side of the subband CRS. This resonance grows in magnitude with increasing FIR energy. (Superposed on this general trend we see some fluctuations perhaps due to filling factor effects.) The growth of the T_3 resonance seems to coincide with a decrease of CR_1. At still higher FIR energies (the trace taken at the 20.12 meV line) we see that CR_1 has disappeared. The T_3 resonance survives, but it decreases in amplitude and increases in linewidth. At the highest FIR energy we see only CR_0.

Further FIR magnetotransmission measurements were performed in order to investigate the evolution of the different resonances with increasing carrier density. The carrier density was changed by controlled pulses of a red LED, and after each light pulse FIR transmission curves were taken at the 12.85 meV and 16.02 meV laser lines. The magnetoresistance was also measured to obtain the relevant subband carrier densities. Figure 3 shows a number of transmission traces taken at the 12.85 meV line. Initially (curve a) a single CR is observed and no second periodicity was observed in the magnetoresistance. The next traces show the appearance of a second CR dip, and this is accompanied by the appearance of a second periodicity in the SdH oscillations. This indicates clearly that the second CR dip originates from the second-subband carriers. After a certain dose of light the onset of parallel conduction was observed. The very sharp T_3 resonance, however, emerged only after a few extra LED bursts, when the parallel conduction had a considerable strength. This suggests some relation between the T_3 resonance and parallel conduction.

From the position of the T_3 resonance as a function of laser energy the effective mass has been extracted. This effective mass is shown in figure 4, together with the effective masses of the subband carriers. It shows a behaviour that is very similar to the cyclotron mass of elec-

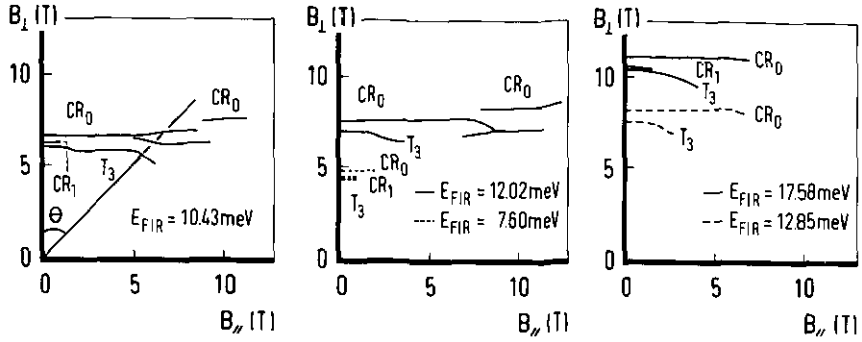

Figure 5. Polar diagrams of the resonance field of the subband CRs and the additional resonance T_3 as a function of tilt angle at several different laser energies: 7.60, 10.43, 12.02, 12.85 and 17.58 meV respectively; sample 2, $N_s = 1.16 \times 10^{16}$ m^{-2}. The tilt angle θ is shown in the leftmost diagram; the total applied field at resonance is given by $B^2 = B_\perp^2 + B_\parallel^2$; 2D behaviour is characterized by $B_\perp$ = constant.

trons in low-carrier-density heterojunctions [9, 10] and bulk GaAs [11, 12]. At energies approaching the energy of the longitudinal optic phonon $\hbar\omega_{LO}$ it shows a strong increase due to the resonant polaron effect [9, 10]. The second-subband effective mass m_1^* is lower than the lowest-subband effective mass m_0^* due to GaAs conduction band non-parabolicity [9]. Band non-parabolicity is also responsible for the approximately linear increase with FIR energy well below $\hbar\omega_{LO}$ of all effective mass values except m_0^*; the latter is approximately constant due to the high density of the lowest-subband carriers [9]. Another effect of the high density of the lowest-subband carriers is the suppression of the resonant polaron effect: the mass does not significantly increase at FIR energies approaching $\hbar\omega_{LO}$. This suppression is due to screening and Landau level occupancy effects [9].

From the SdH spectra the carrier densities have been extracted, and the effective masses and CR linewidths have been obtained from the transmission curves. The two subband effective masses m_0^* and m_1^* tend to increase with total 2DEG sheet carrier density N_s, but beyond a density of $\approx 8.4 \times 10^{15}$ m^{-2} the second-subband mass levels off; at this density also the T_3 resonance begins to appear. The lowest subband CR linewidth shows an approximately linear increase with N_s. This is consistent with the dominance of dielectric broadening of the CR [9, 10].

The position of the T_3 resonance as a function of tilt angle is shown together with the positions of the subband CRs in figure 5. The tilt angle θ is indicated in the leftmost diagram: the applied magnetic field is given by $B = \sqrt{B_\perp^2 + B_\parallel^2}$. The positions at which cyclotron resonances were found for $\approx$ 20 different tilt angles have been plotted in the $B_\perp / B_\parallel$ plane and connected with smooth curves. In these polar plots 2D behaviour will be indicated by straight lines $B_\perp$ = constant, and 3D behaviour by circles B = constant. Three types of resonances were so identified: CR_0, CR_1 and T_3. The position of the T_3 resonance shows 2D behaviour at $E_{FIR} = 7.60$ meV. At higher laser energies it displays 3D behaviour at small tilt angles, but beyond a certain angle the behaviour changes into 2D. The angle at which the crossover occurs increases with increasing laser energy. Not far beyond this angle the T_3 resonance disappears, except at the $E_{FIR} = 10.43$ meV line. At the highest energy ($E_{FIR} = 17.58$ meV) the behaviour is 3D. The kind of behaviour described above has also been observed by Huant *et al* [13] in low-electron-density GaAs–(Ga,Al)As heterojunctions; it has been attributed to subband–Landau-level coupling.

The resonances CR_0 and CR_1 occur at higher values of the perpendicular field component due to the higher effective masses. CR_0 shows 2D behaviour with anticrossings due to higher-order resonant subband–Landau-level coupling [14]. CR_1 is only resolved at very small angles; it shows 2D behaviour at $E_{FIR} = 7.6$ meV and 3D behaviour at $E_{FIR} = 17.58$ meV. This is due to the large spatial extent of the second-subband envelope wavefunction. The mentioned behaviour also indicates that the separation E_{21} between the third and the second subbands is in the range between the two values. This is in agreement with calculations by Ando [15] for a low depletion charge density.

4. Discussion of the origin of the T_3 resonance

In this section we will discuss a number of possible origins of the T_3 resonance. The growth scheme of the samples must be considered to determine which layers in the samples can give rise to this resonance. Figure 6 shows the growth scheme of samples 1, 2 and 3: in these structures all materials are undoped *except* the GaAs cap layer and the Si planar doping in the $Ga_{0.67}Al_{0.33}As$ containing the host donors of the 2DEG. As a result we get a high-density sheet of ionized donors at a distance of 5, 10 or 20 nm from the interface respectively for the samples 1, 2 and 3 [6]. We must now consider which of the layers of the structure of figure 6 (top) can give rise to the T_3 resonance.

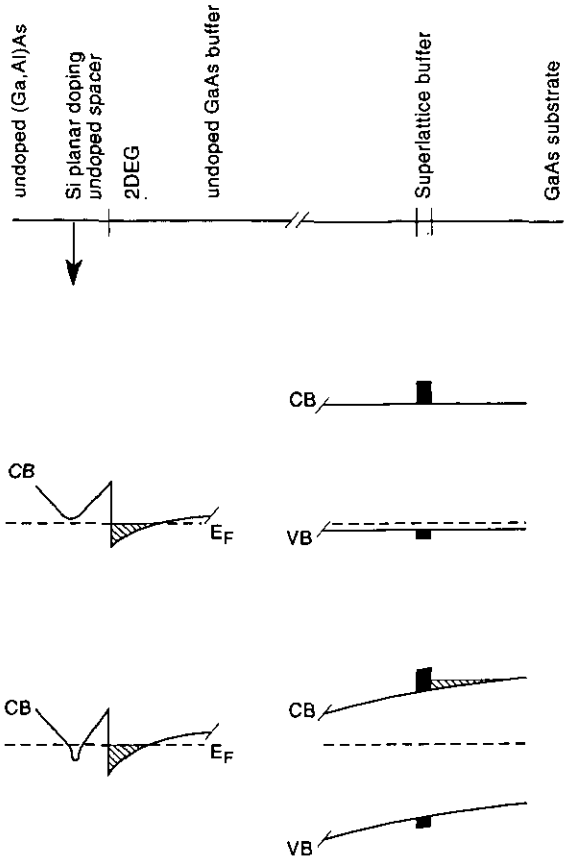

Figure 6. Growth scheme of the heterostructure (top), and spatial dependence of the conduction band potential in the growth direction: (middle) before illumination; (bottom) after saturation of the 2DEG carrier density by bursts of red light, when the depletion width has become so large that it reaches beyond the superlattice buffer.

4.1. Carriers in the (Ga,Al)As layer

Carriers in the (Ga,Al)As layer, which are expected to be responsible for the parallel conduction observed in magnetotransport, have a much higher effective mass value ($m^* \approx 0.088 m_e$ [16]) than electrons in a low-density 2DEG. Furthermore, a linewidth of a few teslas has been observed by Koenraad *et al* [17] in the FIR transmission of a Si δ-doping layer in GaAs. These authors attributed the broadening to the low mobility of the carriers as a result of ionized impurity scattering [18] and to the large carrier density (dielectric broadening [10]). The linewidths observed by Koenraad and co-workers strongly contrast with the linewidths we have found for the T_3 resonance of ≈ 0.06 T. Therefore the conclusion must be that it is very improbable that the T_3 resonance is due to carriers in the (Ga,Al)As layer.

4.2. Bulk GaAs carriers

An alternative explanation of the T_3 resonance is that it could be due to 3D electrons in a GaAs layer of the samples. As the substrate is semi-insulating, the Fermi level is expected to be pinned to deep levels related to residual dopants [19], so that bulk GaAs electrons in the substrate are very unlikely to be the cause of the T_3 resonance. However, the subband occupancies in these samples indicate that they possess an accumulation layer-like character (very low $N_A - N_D$) after illumination with red light ($\hbar\omega > E_g$) [20]. At high carrier densities it might then be possible to get a true accumulation layer with some 3D electrons in the GaAs layer, between the superlattice buffer and the (Ga,Al)As, leading to parallel conduction and the presence of the T_3 resonance. However, the CR of bulk electrons in n-GaAs should be of 3D character, and the resonance field should therefore be completely independent of tilt angle, for all laser energies, in contradiction to the observed tilted-field behaviour. So bulk GaAs electrons are not a probable cause of the T_3 resonance.

4.3. Impurity effects

Fletcher *et al* [21] have suggested that a mobility edge may exist at the bottom of the second subband in GaAs—(Ga,Al)As heterojunctions, below which a tail of localized states is found. As the T_3 resonance has some of the character of an impurity-shifted CR, we consider the possibility of T_3 being associated with Fletcher's localized states. In recent publications different influences of impurities on the FIR response of 2DEG systems have been reported [10, 22–24]. In a magnetic field the localized states would exist at the low-energy sides of the second-subband Landau levels. The energy spread of such a tail would have the correct order of magnitude to lead to a resonance of the localized states which is ≈ 0.25 meV higher in energy than the second subband CR at the same field. However, as the localized states are *lower* in energy than the lowest Landau level of the second subband, they should already be populated at a smaller light dose than that at which second subband occupation occurs. Thus the onset of the T_3 resonance would be expected to occur at a lower light dose than the dose at which the second subband CR becomes observable. As CR_1 is observed *before* T_3 in all experiments in which the light dose (and thus N_s) has been increased, it is unlikely that impurities or localized states associated with E_1 are the origin of the T_3 resonance.

4.4. A (metastable) secondary 2DEG

We suggest that the origin of the additional resonance is a (metastable) shallowly bound 2DEG in a layer behind the superlattice buffer. Such a secondary 2DEG might well be formed as a result of illumination of the sample with red light ($\hbar\omega > E_g$). The physical mechanism might be the following: before illumination of the sample the conduction band is assumed to have the structure shown in the middle diagram of figure 6. In this case, the depletion width is smaller than the thickness of the GaAs buffer layer, so that the band is flat at the position of the GaAs–AlAs superlattice buffer. The electron–hole pairs generated by the first bursts of the red LED recombine in the regions where the conduction and valence bands are flat (among others the superlattice buffer), but are separated and thus

prevented from recombining in the region where the conduction band has a strong slope, i.e. close to and within the depletion region. The electrons move to the 2DEG, thus causing an increase of the carrier density; the holes partly neutralize the ionized acceptors, and this leads to a decrease of the depletion charge density so that the depletion region moves towards the superlattice buffer with further illumination. These processes will cause a decrease of the electric field in the GaAs buffer close to the 2DEG and an increase of the depletion width, since the product of the two is related to the GaAs bandgap [25]. After a certain amount of illumination the depletion region will reach the superlattice buffer. The final situation is shown in the lower diagram of figure 6, where the superlattice buffer is well within the depletion region. Due to the superlattice periodicity, minibands are formed [26, 27], with widths and spacings of the order of 100 meV; the bottom of the lowest miniband is about 100 meV higher than the bottom of the GaAs conduction band [26], and this represents a considerable potential barrier for the CB electrons: combined with the electric field in the depletion layer this forms a secondary potential minimum behind the superlattice. Together these effects produce an accumulation of electrons at the substrate side of the superlattice, and we suggest that the T_3 resonance originates from this electron accumulation layer. Because of the very weak confinement of these electrons a quasi-3D character is displayed, i.e. 2D behaviour at the lower energies, and a gradual transition to 3D behaviour at the highest energies.

The process explained above implies that a large light dose is necessary to observe the T_3 resonance. As a large light dose also leads to parallel conduction in the (Ga,Al)As layer (see section 2), the fact that the T_3 resonance appears after the onset of this type of parallel conduction is coincidental.

The fact that the T_3 resonance is not observed at very low and very high laser energies is expected to be a result of the fact that it becomes indistinguishable from CR of the lowest subband, CR_0.

The effective mass of the T_3 resonance is very similar, both in absolute value and in behaviour, to the cyclotron mass of 2D carriers in low-density GaAs–(Ga,Al)As heterojunctions. As in low-density heterojunctions, the effective mass shows a strong increase at high FIR energies due to the resonant polaron effect [9]. The linewidths of the T_3 resonances are very similar to the values reported in [9, 10]. Thus we conclude that the T_3 resonance behaves as the CR of a low-density 2DEG with a rather high mobility.

Finally, in measurements of the FIR transmission through sample 2 at $N_s = 11.25 \times 10^{15}$ m^{-2} and at $T \approx 20$ K, it appears that the T_3 resonance shows a tendency to decay with time on a timescale of typically several minutes. This indicates a kind of metastability of the secondary 2DEG bound to the superlattice which might be due to electrons tunnelling out through the minibands of the superlattice buffer (via X-conduction band states in the barriers [29]), the process being thermally activated ($k_B T \approx 2$ meV at $T = 20$ K).

5. Summary and conclusions

After a certain dose of illumination with red light ($\hbar\omega > E_g$) parallel conduction is observed in MBE-grown samples with planar Si doping in the (Ga,Al)As. This parallel conduction is due to a large density ($\approx 5 \times 10^{16}$ m^{-2}) of carriers with a low mobility (≈ 0.08 m^2 V^{-1} s^{-1}) after saturation of the carrier density. The origin of this parallel conduction is the δ-doping layer in the (Ga,Al)As.

An additional resonance, denoted as T_3, has been observed in the FIR transmission of two of our samples, after strong illumination with red light. The effective mass extracted from the position of this resonance shows an energy dependence which within experimental accuracy is similar to the energy dependence of the cyclotron mass of electrons in a low-density heterojunction. The resonance is rather narrow, with a linewidth of ≈ 0.06 T, which indicates that the associated carriers have a long relaxation time and a low density. This completely rules out the idea that the electron sheet at the planar Si dopants, responsible for the parallel conduction seen in magnetotransport, is also the cause of the T_3 resonance. Various possible origins of the T_3 resonance were discussed, and the conclusion was reached that there are at least two parallel-conducting layers in our samples: the (Ga,Al)As layer and a layer of electrons near the superlattice buffer. The electrons in this layer are expected to be weakly bound in a shallow potential well formed by the superlattice barrier and the electric field in the depletion region, and are assumed to be the origin of the T_3 resonance. The observed tilted-field behaviour, indicating a transition from 2D to 3D character when the FIR energy increases from 7.6 meV to 17.6 meV, and the fact that the T_3 resonance only appears after the onset of parallel conduction, support this assumption.

Acknowledgments

This work was supported by the Stichting voor Fundamenteel Onderzoek der Materie (FOM) with financial help from the Nederlandse Organisatie voor Wetenschappelijk Onderzoek (NWO). The project was also sponsored by the SCIENCE program of the European Community.

References

[1] Schubert E F, Ploog K, Dämbkes H and Heime K 1984 *Appl. Phys.* A **33** 63

[2] Kirk W P, Kobiela P S, Shih H D and Reed M A 1987 *High Magnetic Fields in Semiconductor Physics (Springer Series in Solid State Sciences vol* 71*)* ed G Landwehr (Berlin: Springer) p 122

[3] Kane M J, Apsley N, Anderson D A, Taylor L L and Kerr T 1985 *J. Phys. C: Solid State Phys.* **18** 5629

[4] Schubert E F, Ploog K, Dämbkes H and Heime K 1984 *Appl. Phys.* A **33** 63

Stormer H L, Gossard A C, Wiegmann W and Baldwin K 1981 *Appl. Phys. Lett.* **39** 912
Kastalsky A and Hwang J C M 1984 *Appl. Phys. Lett.* **44** 333
[5] Maude D K, Portal J C, Dmowski L, Foster F, Eaves L, Nathan M, Heiblum M, Harris J J and Beall R B 1987 *Phys. Rev. Lett.* **59** 815
Chadi D J and Chang K J 1988 *Phys. Rev. Lett.* **61** 873
Lang D V and Logan R A 1977 *Phys. Rev. Lett.* **39** 635
[6] The MBE samples were grown at the Cavendish Laboratory, Cambridge, UK: sample 1, with spacer width 5 nm, was denoted as A227; sample 2, with spacer width 10 nm, as A232; sample 3, with spacer width 20 nm, as A233.
[7] Zrenner A, Koch F, Williams R L, Stradling R A, Ploog K and Weimann G 1988 *Semicond. Sci. Technol.* **3** 1203
[8] Sigg H, Bluyssen H J A and Wyder P 1984 *IEEE J. Quantum Electron.* **20** 616
[9] Langerak C J G M, Singleton J, van der Wel P J, Perenboom J A A J, Barnes D J, Nicholas R J, Hopkins M A and Foxon C T B 1988 *Phys. Rev.* B **38** 13133
[10] Nicholas R J, Hopkins M A, Barnes D J, Brummell M A, Sigg H, Heitmann D, Ensslin K, Harris J J, Foxon C T and Weimann G 1989 *Phys. Rev.* B **39** 10955
[11] Hopkins M A, Nicholas R J, Pfeffer P, Zawadzki W, Gauthier D, Portal J C and DiForte-Poisson M A 1987 *Semicond. Sci. Technol.* **2** 568
[12] Sigg H, Perenboom J A A J, Pfeffer P and Zawadzki W 1987 *Solid State Commun.* **61** 685
[13] Huant S, Grynberg M and Martinez G 1988 *Solid State Commun.* **65** 457
[14] Brummell M A, Hopkins M A, Nicholas R J, Portal J C, Cheng K Y and Cho A Y 1986 *J. Phys. C: Solid State Phys.* **19** L107
[15] Ando T 1982 *J. Phys. Soc. Japan* **51** 3893, 3900
[16] 1982 *Landolt–Börnstein, Numerical Data and Functional Relationships in Science and Technology* vol 17 (Berlin: Springer)
[17] Koenraad P M, Blom F A P, Langerak C J G M, Leys M R, Perenboom J A A J, Singleton J, Spermon S J R M, van der Vleuten W C, Voncken A P J and Wolter J H 1990 *Semicond. Sci. Technol.* **5** 861
[18] van Hall P J, Klaver T and Wolter J H 1988 *Semicond. Sci. Technol.* **3** 120
van Hall P J 1989 *Superlatt. Microstruct.* **6** 213
[19] Holmes D E, Chen R T, Elliott K R and Kirkpatrick C G 1982 *Appl. Phys. Lett.* **40** 46
[20] Harris J J, Lacklison D E, Foxon C T, Selten F M, Suckling A M, Nicholas R J and Barnham K W J 1987 *Semicond. Sci. Technol.* **2** 783
[21] Fletcher R, Zaremba E, D'Iorio M, Foxon C T and Harris J J 1988 *Phys. Rev.* B **38** 7866
[22] Sigg H, Richter J, von Klitzing K and Ploog K 1989 *Spectroscopy of Semiconductor Microstructures (NATO ASI Series B vol* 206*)* ed G Fasol *et al* (London: Plenum) p 471
[23] Ramdas A K and Rodriguez S 1981 *Rep. Prog. Phys.* **44** 1298
[24] Richter J, Sigg H, von Klitzing K and Ploog K 1989 *Phys. Rev.* B **39** 6268
[25] Bastard G 1984 *Surf. Sci.* **142** 284
[26] Maan J C 1984 *Two-Dimensional Systems, Heterostructures and Superlattices (Springer Series in Solid State Sciences vol* 53*)* ed G Bauer *et al* (Berlin: Springer) p 183
[27] Esaki L and Chang L L 1974 *Phys. Rev. Lett.* **33** 495
[28] Merlin R 1987 *Solid State Commun.* **64** 99
[29] Moore K J, Dawson P and Foxon C T 1988 *Phys. Rev.* B **38** 3368